Experimental Investigation and Loss Calculation for a Bi-directional Isolated DC/DC Converter using Series Voltage Compensation

Satoshi Miyawaki
Nagaoka University of Technology
Niigata, Japan
miyawaki@stn.nagaokaut.ac.jp

Jun-ichi Itoh
Nagaoka University of Technology
Niigata, Japan
itoh@vos.nagaokaut.ac.jp

Kazuki Iwaya
TDK-LAMBDA, Ltd
Niigata, Japan
k.iwaya@jp.tdk-lambda.com

***Abstract* – This paper discusses for a bi-directional isolated DC/DC converter using series voltage compensation. The proposed converter consists of a high efficiency resonance full-bridge converter and a series converter. The proposed circuit regulates the output voltage by using the series converter, which provides only the differential voltage between the input voltage and the output voltage that is closed to the nominal voltage, since only the resonance converter will operate. In this paper, four types of the auxiliary circuits are investigated using the loss calculation. The relationship between the loss element and efficiency characteristics is clarified. The validity of the proposed circuit was confirmed by experimental results, which converts 48-V to 380-V at 1kW, with a maximum efficiency of 95% at 1 kW at the nominal input voltage region.**

I. INTRODUCTION

Recently, high efficiency and high power density bi-directional isolated DC/DC converters are increasingly desired in the application of power grid system that found in the smart grid system and electric vehicles. Examples of the applications of the DC/DC converters are such as the secondary battery conversion for photovoltaic cell and also power conditioner for fuel cell. In addition, these power converters have to control a wide range of output voltage [1-10].

The series resonant type full-bridge converters, which use a resonance between the leakage inductance of transformers and the series resonant capacitor, are one of the most effective circuit topologies to achieve high efficiency. However, it is difficult to regulate the output voltage in a wide range while there is a fluctuation in the input voltage because the switching timing is constrained by the resonance period. Although the voltage is controllable by using the series resonant converter, If it has a wide voltage control range, this converter has some problem, such as increasing reflux current and difficult design of a transformer [11-14].Therefore, a series resonant type full-bridge converter is connected to a voltage control converter, such as a step down chopper [15-17]. As a result, the converter loss will increase because all the power passes through two converters.

In the power grid system, series voltage compensation is used in order to compensate the grid voltage [18][19].Furthermore, the non-isolated DC-DC converters using series voltage compensation have also proposed and discussed on the voltage fluctuation [20][21]. In this system, the auxiliary converter is connected in series to the power supply. As a result, the power rating of the converter is low and high efficiency is achievable.

The authors previously have proposed the isolated DC/DC converter using the series voltage compensation [22][23]. The input voltage fluctuation is compensated by the auxiliary circuit that outputs only the fluctuation of the output voltage. One of the advantages of the proposed circuit is that high efficiency can be achieved when the input voltage is closed to the nominal input voltage because the power of the auxiliary circuit becomes very small in comparison to the input power. Normally, the large fluctuations do not occur in the input or the output voltage for long periods, and as a result, the converter loss can be reduced. However, the previous works have only discussed on single direction of s energy flow. Bidirectional flow of energy in the proposed DC/DC converter, including the effectiveness of the auxiliary circuit has not been evaluated.

This paper discusses and evaluates the losses of the bi-directional isolated DC/DC converter using series voltage compensation. In order to achieve the high efficiency, four types of the auxiliary circuits are investigated and it is necessary to clarify the procedure of optimize design in subjects to the efficiency characteristics. The first section of this paper introduces the principle of the proposed series compensation method. Secondary, expression for the converter loss is established in order to estimate the power loss. The point of the expression for the converter loss is to observe the losses of a converter based on the device conditions. Thirdly, the proposed calculation method that is used to evaluate the power loss is confirmed with the experimental results. Finally, experimental results demonstrate the advantages of the proposed converter.

II. CIRCUIT CONFIGURATIONS

A. Conventional Circuit

Fig. 1 shows the power flow diagram of the conventional converter, which is composed form a series connection of series resonant converter and voltage control converter, such as a step down chopper [15-17]. The series resonant converter operates at constant duty cycle based on the resonance frequency f_0, and does not control the output voltage. The fluctuation of the input voltage is constantly controlled by the chopper circuit. The output side is isolated by the resonant converter to the input side. This system has two stages of power flow from the input to the output. The total efficiency of the conventional circuit η_c is obtained from Eq.(1), using both the resonant converter efficiency η_r and the buck chopper efficiency η_{chop}.

$$\eta_c = \eta_r \eta_{chop} \tag{1}$$

As a result, all the power passes through both converters despites of the relation with the input voltages; therefore, the converter efficiency is reduced.

B. Proposed Circuit

Fig. 2 shows the power flow diagram of the proposed converter. In the proposed circuit, the resonant converter is used in the main circuit for voltage isolation. In order to achieve the high efficiency, the resonant converter operates at constant duty cycle based on the resonance frequency f_0. In addition, the auxiliary circuit is used to regulate the output voltage. The output voltage of the auxiliary circuit is added to the output of the main circuit by a transformer. Therefore, the auxiliary circuit compensates only the fluctuation voltage, against the output voltage commands.

The proposed system consists of two power converters, which are connected in series to the output side. The reason for high efficiency is as follows. The power P_{out} is obtained by

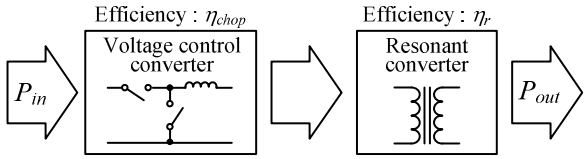

Fig. 1. Power flow diagram of the conventional circuit using a chopper circuit and a resonant converter.

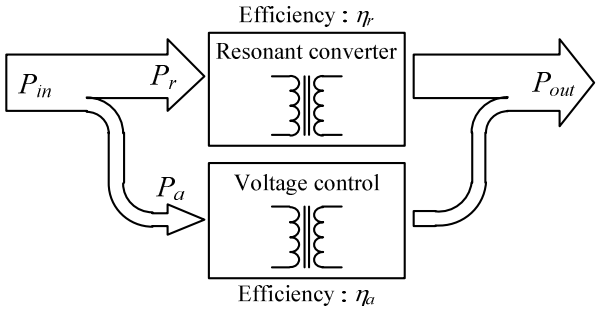

Fig. 2. Power flow diagram of the isolated DC/DC converter using the series voltage compensation.

adding the auxiliary converter power P_a to the directly power P_r. The total converter efficiency of the proposed circuit η_p is obtained by Eq.(2), using the auxiliary circuit efficiency η_a and the power ratio $k=P_a/P_r$.

$$\eta_p = \frac{\eta_r + k\eta_a}{1+k} \tag{2}$$

Therefore, the total efficiency η_p of the proposed circuit is higher than the conventional circuit where the efficiency can be expressed by Eq. (3). It should be noted that the series efficiency of the resonant converter in the conventional circuit is similar to the proposed circuit.

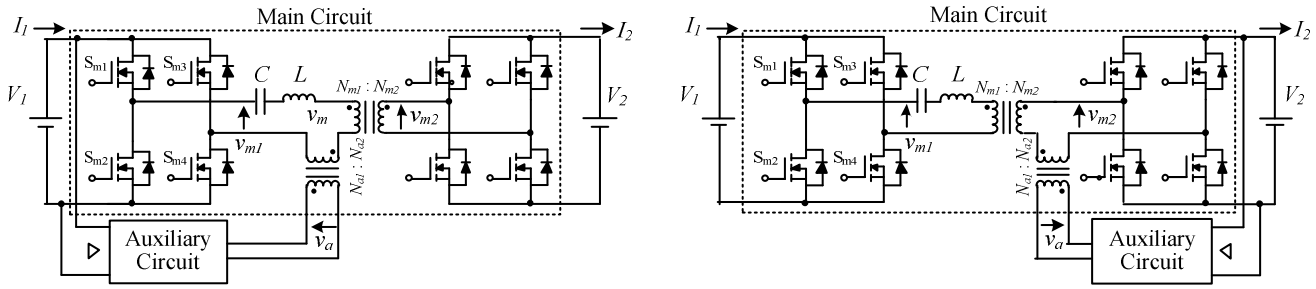

(a) Primary compensation. (b) Secondary compensation.

Fig. 3. Circuit diagrams of the proposed circuit.

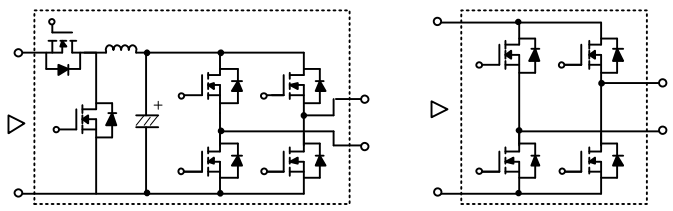

(a) Step down chopper + Full-bridge. (b) Full-bridge.

Fig. 4. Circuit diagrams of the auxiliary circuit.

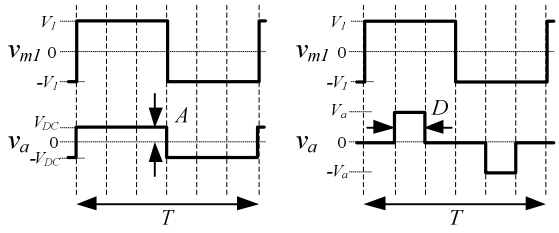

(a) Step down chopper + Full-bridge. (b) Full-bridge.

Fig. 5. Voltage waveforms of the proposed circuit.

$$\frac{\eta_r + k\eta_a}{1+k} > \eta_r \eta_{chop} \tag{3}$$

Fig. 3 shows the proposed circuit using the series voltage compensation. The main circuit is controlled under an optimum condition similar to the resonant converter. In order to obtain the maximum efficiency, the resonant converter operates at 50% duty cycle based on the resonance frequency f_0. Therefore, the main circuit can achieve zero current switching (ZCS) at any time. The resonance frequency of the proposed circuit f_0 is obtained by Eq. (4) using the resonant capacitor C and the resonant inductance L that is containing the leakage inductance of the transformers.

$$f_0 = \frac{1}{2\pi\sqrt{LC}} \tag{4}$$

Moreover, the auxiliary circuit can be connected to either primary side or secondary side of the main circuit as shown in Fig. 3. Fig. 3(a) shows the circuit configuration that the auxiliary circuit connects to the primary side. On the other hand, Fig. 3(b) shows a circuit configuration that the auxiliary circuit connects to the secondary side.

Fig. 4 shows the circuit configuration of the auxiliary circuit. Fig. 5 shows the voltage waveforms when the auxiliary circuit is connected with the primary side.

Fig. 4(a) shows the circuit configuration of the series connection of the step down chopper and full-bridge converter. In this circuit, the switching timing of the auxiliary circuit is synchronous with the main circuit. Then, the output voltage is controlled by changing the DC link voltage between the step down chopper and full bridge converter. The high efficiency can be achieved by using the high speed switching devices for the step down chopper and low on-resistance switching devices for the full-bridge converter. However, the number of the switching device is increased.

Fig. 4(b) shows the full-bridge converter is used for the auxiliary circuit. In this circuit, the auxiliary circuit can output three different voltage levels; $+V$, $-V$, and zero voltage. The output voltage is controlled by changing the pulse width D of the auxiliary circuit. The number of the switching device is decreased. However, the switching loss of the MOSFET is increased, and the control becomes complicated.

III. Explessions for Power Loss

This section explains the power loss expression of the proposed circuit. The power loss of the proposed circuit is separated into the main circuit loss and auxiliary circuit loss. In the main circuit, the switching loss is ideally zero, because the switching devices can achieve ZCS. Therefore, the power loss of the main circuit consists of the conduction loss and constant loss. The conduction loss is generated in the on-resistance of the FET, wire resistance of the transformer, and the equivalent series resistance of the capacitor. The constant loss is generated within the iron-loss of the transformer, and no-load loss. On the other hand, the power loss of the auxiliary circuit consists of the conduction loss, constant loss, and switching loss which are generated at the switching period, from the forward voltage drop of a switching device, respectively. It should be noted that the following expression is referred to the case of Fig. 3(a).

A. FET Loss in Main Circuit

The resonant current of the proposed circuit is a sinusoidal waveform, provided that the resonant parameter of the proposed circuit is optimally designed [18][19]. Therefore, the power loss per primary FET in the main circuit $P_{loss\_FET\_main1}$ can be obtained by Eq. (5) using the on-resistance of the FET $R_{on\_FET\_main1}$. Thus, the power loss per secondary FET in the main circuit $P_{loss\_FET\_main2}$ can be obtained by Eq. (6) using the on-resistance of the FET $R_{on\_FET\_main2}$.

$$P_{loss\_FET\_main1} = \frac{\pi^2}{8} R_{on\_FET\_main1} {I_1}^2 \tag{5}$$

$$P_{loss\_FET\_main2} = \frac{\pi^2}{8} R_{on\_FET\_main2} {I_2}^2 \tag{6}$$

B. FET Loss in Auxiliary Circuit I

The power loss of the auxiliary circuit FET consists of the conduction loss and switching loss. In the auxiliary circuit of Fig. 4(a), the conduction loss of the chopper FET $P_{loss\_FET\_chop\_con}$ can be obtained by Eq. (7) using the on-resistance of the chopper FET R_{on_chop} and the turn ratio of the transformer in the auxiliary circuit, which is $\beta = N_{a1}/N_{a2}$.

$$P_{loss\_FET\_chop\_con} = R_{on\_chop} (\beta I_1)^2 \tag{7}$$

In addition, the switching loss of the FET is proportional to the applied voltage and current. Therefore, the switching loss of the chopper $P_{loss\_FET\_chop\_sw}$ can be obtained from Eq. (8).

$$P_{loss\_FET\_chop\_sw} = V_1 (\beta I_1)(e_{on} + e_{off}) f_{sw} \tag{8}$$

where e_{on}[J] and e_{off}[J] are the turn-on and turn-off energy at per switching, and f_{sw} is the switching frequency. In the full bridge converter, the switching loss is ideally zero since the the FET achieves ZCS. Therefore, the power loss per FET in the full bridge $P_{loss\_FET\_FB}$ can be obtained by Eq. (9) using the on-resistance of the FET $R_{on\_FET\_FB}$.

$$P_{loss\_FET\_FB} = \frac{\pi^2}{8} R_{on\_FB} (\beta I_1)^2 \tag{9}$$

C. FET Loss in Auxiliary Circuit II

In the auxiliary circuit of Fig. 4(b), the conduction loss can be expressed as Eq. (9), similarly to the case of Fig. 4(a). The switching loss of the full-bridge converter is obtained by Eq. (10) due to the sinusoidal waveform.

$$P_{loss\_FET\_FB\_sw} = \frac{\pi}{2} (\beta I_1) V_1 (e_{on} + e_{off}) f_{sw} \sin\left\{\frac{\pi}{2}(1 - f_{sw} t_{on})\right\} \tag{10}$$

where t_{on} is the compensation time per one cycle of the auxiliary circuit.

D. Capacitor Loss

The capacitor loss is calculated based on the capacitor current during the charge or discharge, equivalent series resistance of the capacitor. The resonant capacitor loss $P_{loss\_C\_reso}$ is obtained by Eq. (11) using the equivalent series resistance R_{C_reso}.

$$P_{loss\_C\_reso} = \frac{\pi^2}{8} R_{C\_reso} I_1^2 \tag{11}$$

The current based on the mean value of the sine wave is charged or discharged to the output capacitor. Therefore, the output capacitor loss $P_{loss\_C\_out}$ is obtained by Eq. (12) using the equivalent series resistance R_{C_out}.

$$P_{loss\_C\_out} = \left\{ \frac{\pi^2}{8} - 1 \right\} R_{C\_out} I_2^2 \tag{12}$$

E. Transformer Loss

The power loss of transformer consists of the iron loss and copper loss. The iron loss is occurring because of the flux change in the core. The copper loss is occurring in the winding resistance of transformer. At first, when the square wave is inputted to the transformer, the flux density B_{ac} is obtained by Eq. (13).

$$B_{ac} = \frac{V_{N1} \cdot t_{on}}{2 N_1 A_c} \tag{13}$$

where V_{N1} is the primary voltage of the transformer, N_1 is the primary wire turns, A_c[m^2] is the effective cross-section of the core. Therefore, the iron loss of the transformer P_{trans_fe} is obtained by Eq. (14) using the characteristics of the flux density - core loss value P_{cv}[W/m^3] and the effective volume of the core V_e[m^3].

$$P_{trans\_fe} = P_{cv} V_e \tag{14}$$

The copper loss of the transformer is obtained from the winding resistance with skin effect. The primary winding copper loss P_{loss_Nm1} in the main circuit is obtained by Eq. (15) using the primary winding resistance of the main circuit with skin effect R_{N1_main}. The secondary winding copper loss P_{loss_Nm2} in the main circuit is obtained by Eq. (16) using the primary winding resistance of the main circuit with skin effect R_{N2_main}. The transformer loss of the auxiliary circuit is obtained similarly.

$$P_{loss\_Nm1} = \frac{\pi^2}{8} R_{N1\_main} I_1^2 \tag{15}$$

$$P_{loss\_Nm2} = \frac{\pi^2}{8} R_{N2\_main} I_2^2 \tag{16}$$

Table 1. Specification parameters of the power loss calculation for bi-directional isolated DC/DC converter.

Element	Symbol	Value
Input voltage	V_1	36 ~ 60 V (typ. 48 V)
Output voltage	V_2	284 ~ 476 V (typ. 380 V)
Rating power	P_{out}	1000 W
Switching frequency	f_{sw}	100 kHz
Wire turns (main trans.)	N_{m1} : N_{m2}	1 : 8
Wire turns (auxiliary trans.)	N_{a1} : N_{a2}	2 : 1

F. Series inductor loss

The power loss of series resonant inductor consists of the iron loss and copper loss as well as the transformer loss. The copper loss is obtained from the winding resistance similar to the Eq. (15) and Eq. (16).

In the iron loss, the series inductor voltage is obtained at first. Then, the flux density is obtained by Eq. (13) as well as the transformer, and iron loss is calculated from a core loss value. The peak value of the series inductor voltage is obtained by Eq. (17).

$$V_{L\_peak} = 2\pi f_0 L \cdot \frac{\pi}{2} I_1 \tag{17}$$

IV. Efficiency Estimation by Loss Calculation

A. Efficiency Estimation of proposed converter

Four types of the auxiliary circuits shown in Fig. 3 and Fig. 4 are investigated using the loss calculation. The circuit parameters are shown in Table 1. The rating power is 1 kW. The primary voltage has a fluctuation of 48 V ± 25%, and the secondary voltage has a fluctuation of 380 V ± 25%. Fig. 6 demonstrates the efficiency of the proposed converter at a constant load and a constant secondary voltage 380 V when the primary voltage has a fluctuation. On the other hands, Fig. 7 presents the efficiency at a constant load and a constant primary voltage 48 V when the secondary voltage is fluctuating.

From the calculation results, a maximum efficiency of over 94.0% is obtained in all cases. In addition, the high efficiency in a wide range can be achieved when the voltage fluctuation is compensated from the voltage changing side (In Fig. 6(a) and (c), the primary side voltage changes while the secondary side voltage is constant. In Fig. 7(b) and (d), the secondary side voltage changes while the primary side voltage is constant.). The efficiency is decreased when the voltage fluctuation is compensated from the side that the voltage is unchanged side (Fig. 6(b), (d) and Fig. 7(a), (c)) the efficieny is decreased due to the difference in the power flow at the boost and buck mode. When the efficiency is decreased, the circulation current between the auxiliary circuit and the main circuit is increased. Therefore, the loss of the power circuit is further decreased when it connects the auxiliary circuit that regulates with larger voltage fluctuation.

Moreover, when the configuration of the auxiliary circuit composed from the chopper and full-bridge, the conduction loss will be increased. Therefore, to obtain the high efficiency, the auxiliary circuit is connected with a high voltage side. On

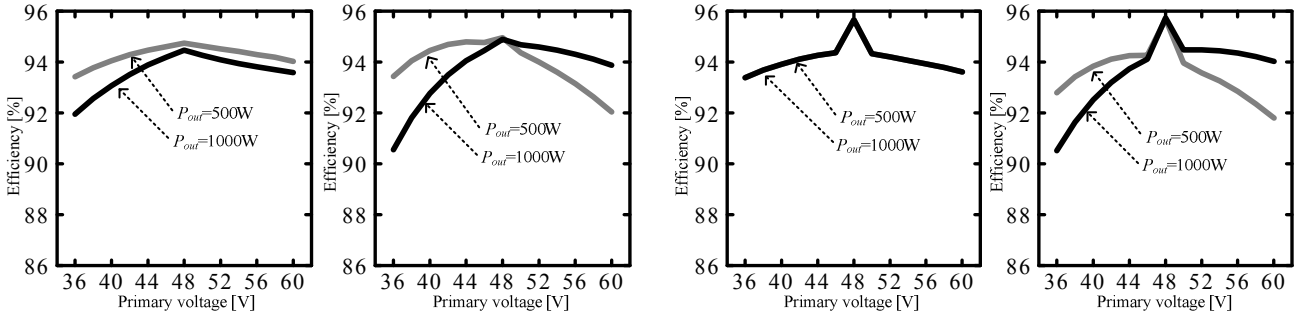

(a) Primary compensation. Step down chopper + Full-bridge. (b) Secondary compensation. Step down chopper + Full-bridge. (c) Primary compensation. Full-bridge. (d) Secondary compensation. Full-bridge.

Fig. 6. Calculation results of the primary voltage compensation (V_1=48V±25%, V_2=380V).

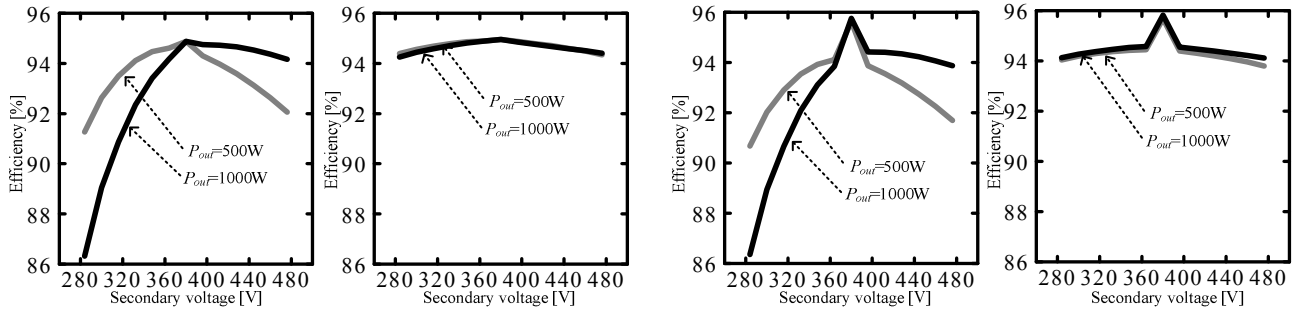

(a) Primary compensation. Step down chopper + Full-bridge. (b) Secondary compensation. Step down chopper + Full-bridge. (c) Primary compensation. Full-bridge. (d) Secondary compensation. Full-bridge.

Fig. 7. Calculation results of the secondary voltage compensation (V_1=48V, V_2=380V±25%).

the other hands, when the auxiliary circuit configuration is only composed by a full-bridge, the switching loss will be increased. Therefore, the auxiliary circuit is connected at the low voltage side in order to obtain high efficiency.

Therefore, in order to achieve the high efficiency, the circuit configuration must fulfill the following conditions.

(1) It connects the auxiliary circuit to the side that has the large voltage fluctuation side

(2) The auxiliary circuit which connects chopper and full-bridge is connected to the high voltage side, and the auxiliary circuit which only composed by a full-bridge is connected to the low voltage side.

B. Determination of Circuit Configuration

Assuming that the primary side is connected to a side that has large fluctuation voltage such as the battery (48 V) and the secondary side is low fluctuation range like the DC bus voltage (380 V).

Then, the power loss can be reduced by connecting the auxiliary circuit to the primary side, because the primary side has large fluctuation voltage. In addition, the auxiliary circuit configuration is a full-bridge circuit only since the primary side has low voltage.

The experimental circuit configuration is a combination of the full-bridge converter with the primary side compensation. (Fig. 3(a) and Fig. 4(b)). In this case, the battery voltage has a large fluctuation. In addition, to obtain high efficiency, the auxiliary circuit is connected to the low voltage side.

V. EXPRIMENTAL RESULTS

The proposed converter was tested for validation. It is assumed that the primary side is connected to the battery (48 V ± 25%), and the secondary side is connected to the DC bus (constant 380 V).

At first, the experimental results of the main circuit are presented in order to confirm the high efficiency can be achieved in the main circuit. Then, experimental results of the proposed circuit are presented at the second.

A. Experimental results of the main circuit

Fig. 8 shows the load characteristics of the main circuit. In this experiment, the auxiliary circuit is not operated. The power flows from a primary side to the secondary side. The turn ratio of the transformer in the main circuit is 1:8. Therefore, the secondary voltage becomes 380V when the primary voltage of the main circuit is closed to 48V as shown in Fig. 8. However, the control method is an open-loop control, that is, the duty cycle is set to 50%.

As a result, the maximum efficiency of 95.5% is obtained at load of 650 W, as shown in Fig. 8. It is confirmed that the high efficiency is achieved in the main circuit.

B. Experimental results of the proposed circuit

Fig. 9 presents the efficiency of the proposed converter at a constant load and constant secondary voltage 380 V when the primary voltage has fluctuation of ±25%. The maximum efficiency of 95.5% is obtained, when the primary voltage is closed to the nominal primary voltage (48 V). In both boost

and step down modes, it was confirmed that the voltage control can be regulated while maintaining high efficiency.

Fig. 10 presents the primary current of the main transformer and the terminal voltage of S_{m2}. In the following orders, the maximum efficiency condition (The auxiliary circuit is not operated). Also, the full-bridge converter is controlled to achieve ZCS.In the boost and buck modes Also, the full-bridge converter is controlled to achieve ZCS. The switching frequency is approximately 100 kHz was confirmed.

Fig. 11 presents the AC voltage waveforms of the each circuit. In both boost and step down modes, the auxiliary circuit outputs three different voltage levels; $+V_1$, $-V_2$, and zero voltage. When the input voltage is decreased (Fig. 14(b)), the auxiliary circuit outputs a positive phase voltage to the main circuit without preventing the resonance operation of the main converter. Similarly, when the input voltage is increased (Fig. 14(c)), the auxiliary circuit outputs a negative phase voltage.

C. Converter Loss breakdown

Fig. 12 presents the breakdown of the prototype losses. The iron loss in the main transformer is predominant. In order to clarify the power loss of the proposed circuit, the loss measurement and analysis for each of the part have been examined using expression in chapter 3. Additionally, the power loss of the main transformer is predominant, it account for 15% of the total loss. The auxiliary FET loss increases in both boost and buck modes. Therefore, in order to obtain higher efficiency, it is necessary to optimize the transformer design, and the selection of FETs in the auxiliary circuit is important. The low on-state resistance device should be chosen because the voltage rating of the FET can be reduced in comparison with the main circuit.

VI. CONCLUSION

This paper proposed a bi-directional isolated DC/DC converter using series voltage compensation which consisting of a series resonant type full-bridge converter and an auxiliary converter. The concept of the series compensation is that the changing side voltage is regulated by adding or subtracting the auxiliary converter voltage to the series resonant type full-bridge voltage.

Four types of the proposed circuit are investigated and evaluated in term of losses. The relationship between the loss elements and efficiency characteristics are clarified. The expressions for the power loss are established and evaluated. The validity of the loss calculation was confirmed theoretically with a efficiency of over 94% with wide voltage control range at 1 kW.

The experimental results confirmed that the maximum efficiency of 94.5% at 1 kW is obtained when the primary voltage was closed to the nominal primary voltage. It was confirmed that the voltage control can be regulated while maintaining high efficiency. From the loss analysis, it can notice that, the power loss of the main transformer is predominant.

In future work, the converter efficiency will be improved by the optimizing the design, the converter efficiency will be

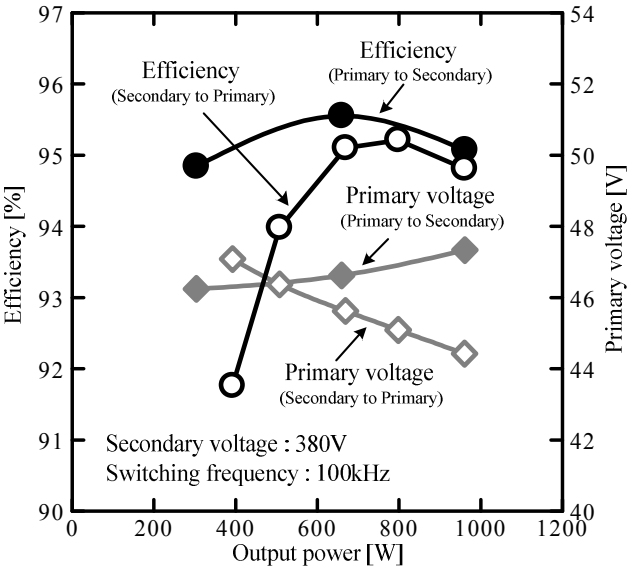

Fig. 8. Experimental results of the load characteristics only the main circuit.

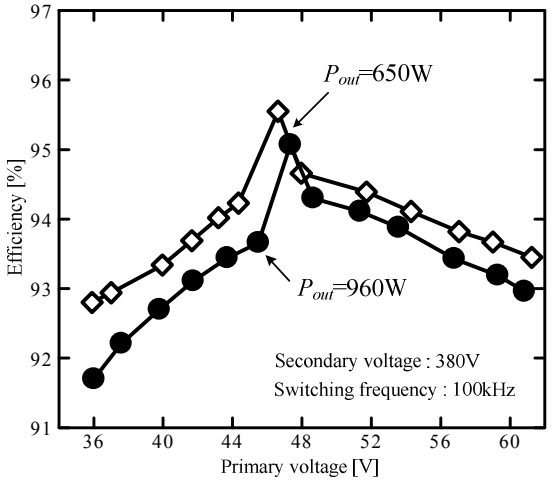

(a) Primary to Secondary.

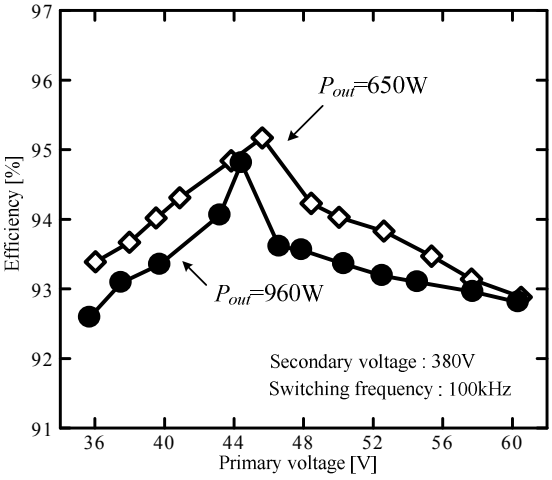

(b) Secondary to Primary.

Fig. 9. Experimental results of the primary voltage compensation of the proposed circuit.

evaluated with a higher conversion capacity, also evaluated with other circuit configuration patterns.

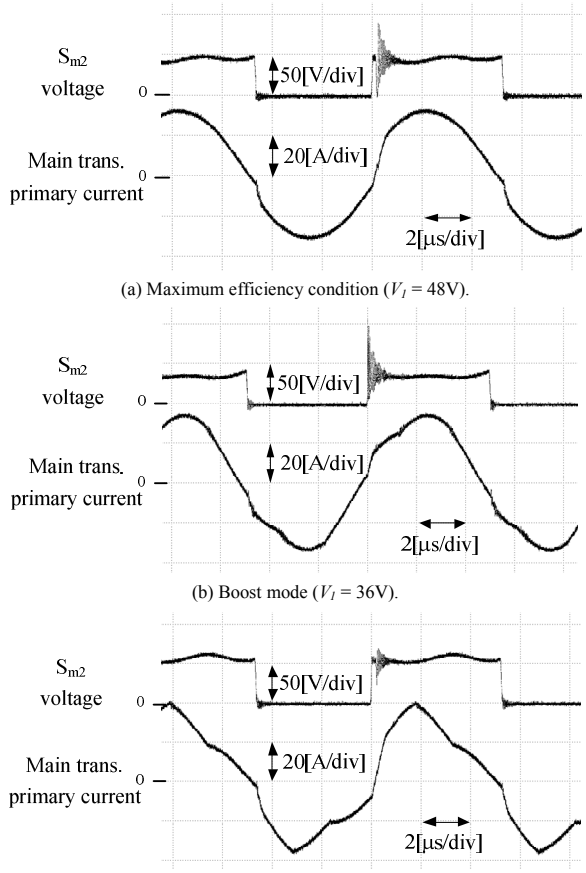

(a) Maximum efficiency condition (V_I = 48V).

(b) Boost mode (V_I = 36V).

(c) Step down mode (V_I = 60V).

Fig. 10. Waveforms of the main transformer primary current and the terminal voltage of S_{m2} (P_{out}=960W).

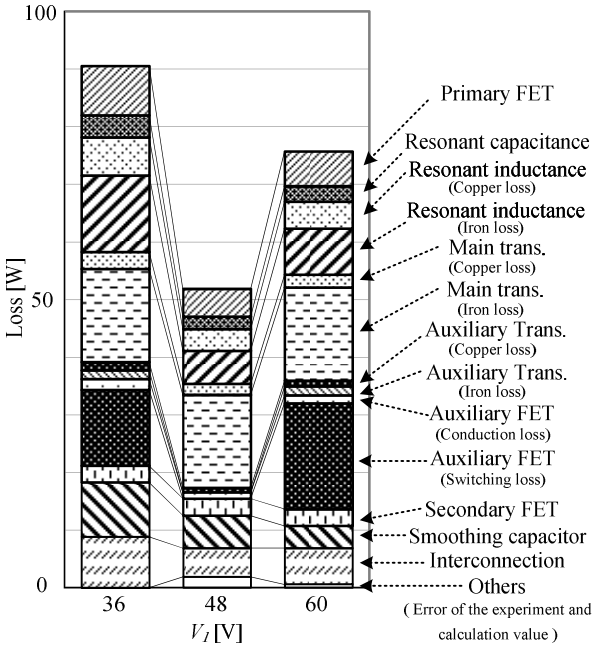

Fig. 12. Loss partition results of a prototype.

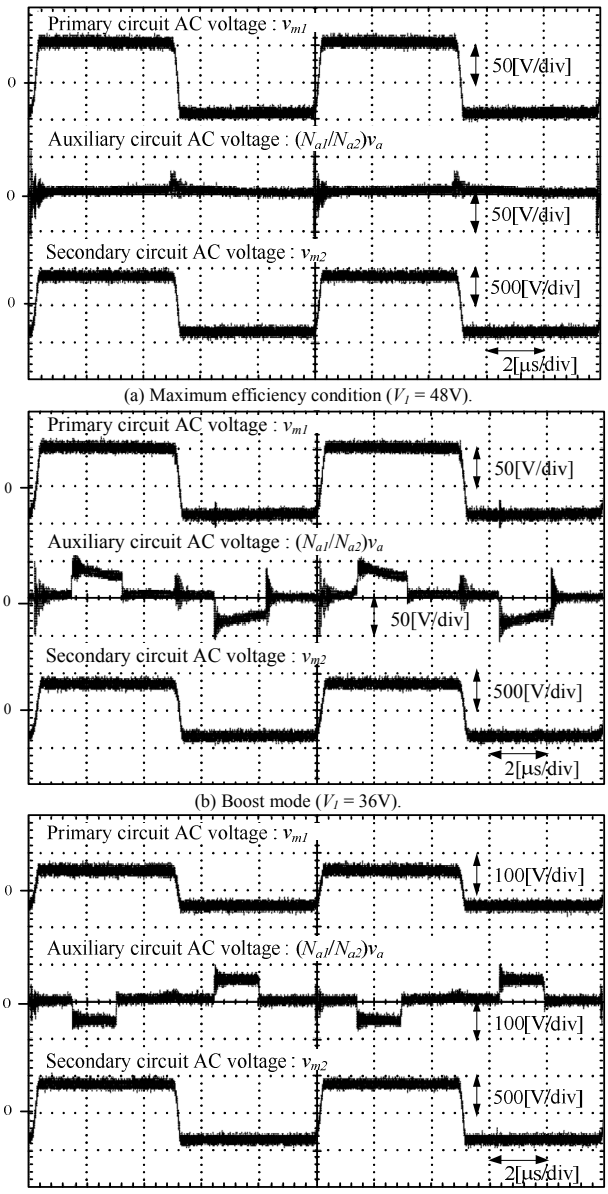

(a) Maximum efficiency condition (V_I = 48V).

(b) Boost mode (V_I = 36V).

(c) Step down mode (V_I = 60V).

Fig. 11. AC voltage waveforms of the each circuit (P_{out}=960W).

REFERENCES

[1] Krismer. F, Biela. J, Kolar. J. W, : "A comparative Evaluation of Isolated Bi-directional DC/DC Converters with Wide Input and Output Voltage Range", Industry Applications Conference 2005, pp.599-606, 2005.

[2] S. Inoue, H. Akagi : "A Bi-directional DC/DC Converter for an Energy Storage System", Applied Power Electronics Conference, APEC 2007 - Twenty Second Annual IEEE,, pp.761-767, 2007.

[3] Du, Yu ; Lukic, Srdjan ; Jacobson, Boris ; Huang, Alex : "Review of high power isolated bi-directional DC-DC converters for PHEV/EV DC charging infrastructure", Energy Conversion Congress and Exposition (ECCE) 2011, pp.553-560, 2011

[4] T. F. Wu, J. G. Yang, C. L. Kuo, S. Z. Lan : "Isolated Bi-Directional Full-Bridge Soft-Switching DC-DC Converter with Active and Passive Snubbers", Applied Power Electronics Conference and Exposition (APEC) 2011, pp.844-850 , 2011.

[5] D. Aggeler, J. Biela, S. Inoue, H. Akagi, J.W. Kolar : "Bi-Directional Isolated DC-DC Converter for Next-Generation Power Distribution - Comparison of Converters using Si and SiC Devices", Power Conversion Conference - Nagoya, 2007, pp.510-517, 2007.

[6] J.Biela, U.Badstuebner, J.W.Kolar : "Impact of Power Density Maximization on Efficiency of DC-DC Converter Systems", IEEE Transaction on Power Electronics, Vol. 24, No. 1, pp.288-300, 2009.

[7] K.Fathy, K.Morimoto, T.Doi, H.Ogiwara, H.W.Lee, M.Nakaoka : "A Diveided Voltage Half-Bridge High Frequency Soft-Switching PWM DC-DC Converter with High and Low Side DC Rail Active Edge Resonant Snubbers", IPEMC 2006, Vol. 2, pp.1-5, 2006.

[8] M.N. Kheraluwala, R.W. Gascoigne, D.M. Divan, E.D. Baumann : "Performance characterization of a high-power dual active bridge DC-to-DC converter", Industry Applications, IEEE Transactions on Volume 28, Issue 6, pp.1294-1301, 1992.

[9] Kheraluwala M.N., Gascoigne R.W., Divan D.M., Baumann E.D. : "Performance Characterization of a High-Power Dual Active Bridge DC-to-DC Converter", IEEE Transactions on Industry Applications, Volume 28, Issue 6, pp.1294-1301, 1992.

[10] Hui Li, Fang Zheng Peng, Lawler J.S. : "A natural ZVS medium-power bidirectional DC-DC converter with minimum number of devices", Industry Applications, IEEE Transactions on Volume 39, Issue 2, pp.525-535, 2003.

[11] R. L. Steigerwald : "A Comparison of Half-Bridge Resonant Converter Topologies", IEEE Trans. on Power Electronics, Vol. 3, No. 2, pp.174–182, 1988.

[12] A. K. S. Bhat : "Analysis and design of LCL-type series resonant converter", IEEE Trans. on Industrial Electronics, Vol. 41, No. 1, pp.118–124, 1994.

[13] G. Raju, S. Doradla : "An LCL reosnant converter with PWM control-analysis, simulation and implementation", IEEE Trans. on Power Electronics, Vol. 10, No. 2, pp.164–174, 1995.

[14] J.F. Lazar, R. Martinelli : "Steady-State Analysis of the LLC Series Resonant Converter", Applied Power Electronics Conference and Exposition, 2001. APEC 2001. Sixteenth Annual IEEE, Vol. 2, pp.728-735, 2001.

[15] M.Takagi, K.Shimizu, T.Zaitsu, "Ultra High Efficiency of 95% for DC/DC Converter - Considering Theoretical Limitation of Efficiency", IEEE APEC 2002, vol. 2, pp. 735-741, 2002.

[16] P.Alou, J.Oliver, J.A.Cobos, O.Garcia, J.Uceda, "Buck+half bridge (d=50%) topology applied to very low voltage power converters", APEC 2001, Sixteenth Annual IEEE Volume 2, pp 715-721, 2001.

[17] T. Qian, B. Lehman : "Buck/Half-Bridge Input-Series Two-Stage Converter", Power Electronics, IET Volume 3, Issue 6 , pp.965-976, 2010.

[18] J.D. Barros, J.F. Silva : "Multilevel Optimal Predictive Dynamic Voltage Restorer", IEEE Transactions on Industrial Electronics Volume 57, Issue 8, pp.2747-2760 (2010)

[19] T. Jimichi, H. Fujita, H. Akagi : "Design and experimentation of a dynamic voltage restorer capable of significantly reducing an energy storage element", IEEE Transactions on Industry Applications, Vol. 44, No. 3, pp.817–825 (2008)

[20] Giuseppe Guidi, Tore M. Undeland, Yoichi Hori : "An Interface Converter with Reduced VA Ratings for Battery-Supercapacitor Mixed Systems", Power Conversion Conference - Nagoya 2007, pp.936-941, 2007.

[21] Jong-Pil Lee, Byung-Duk Min, Dong-Wook Yoo, Tae-Jin Kim, Ji-Yoon Yoo :"A new topology for PV DC/DC converter with high efficiency under wide load range", Power Electronics and Applications 2007 European Conference, pp1-6, 2007.

[22] S. Miyawaki, J. Itoh, K. Iwaya :"High Efficiency Isolated DC/DC Converter Using Series Voltage Compensation", IEEJ, Vol.130-D, No.1, pp.43-50, 2010. (in Japanese)

[23] S. Miyawaki, J. Itoh, K. Iwaya :"High Efficiency Isolated DC/DC Converter using Series Connection on Secondary Side", IEEJ, Vol.131-D, No.10, pp.1175-1183, 2011. (in Japanese)